AD-A143 966 NONLOCAL EFFECTS ON THE CONVECTIVE PROPERTIES OF THE ELECTROSTATIC CURREN..(U) NAVAL RESEARCH LAB WASHINGTON DC G GANGULI ET AL. 27 JUL 84 NRL-MR-5372 1/1

UNCLASSIFIED F/G 20/7 NL

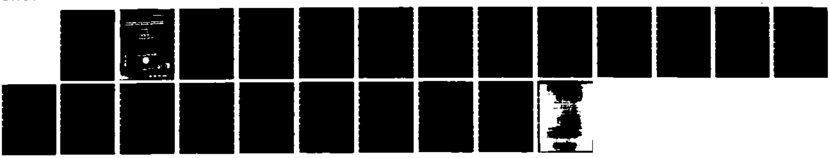

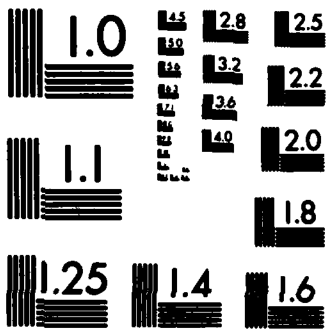

MICROCOPY RESOLUTION TEST CHART
NATIONAL BUREAU OF STANDARDS-1963-A

AD-A143 966

SECURITY CLASSIFICATION OF THIS PAGE

REPORT DOCUMENTATION PAGE

1a REPORT SECURITY CLASSIFICATION UNCLASSIFIED	1b RESTRICTIVE MARKINGS
2a SECURITY CLASSIFICATION AUTHORITY	3 DISTRIBUTION/AVAILABILITY OF REPORT Approved for public release; distribution unlimited.
2b DECLASSIFICATION/DOWNGRADING SCHEDULE	
4 PERFORMING ORGANIZATION REPORT NUMBER(S) NRL Memorandum Report 5372	5. MONITORING ORGANIZATION REPORT NUMBER(S)
6a NAME OF PERFORMING ORGANIZATION Naval Research Laboratory 6b. OFFICE SYMBOL (If applicable) Code 4780	7a. NAME OF MONITORING ORGANIZATION
6c ADDRESS (City, State and ZIP Code) Washington, DC 20375	7b. ADDRESS (City, State and ZIP Code)
8a. NAME OF FUNDING/SPONSORING ORGANIZATION ONR and NASA 8b OFFICE SYMBOL (If applicable)	9. PROCUREMENT INSTRUMENT IDENTIFICATION NUMBER
8c ADDRESS (City, State and ZIP Code) Arlington, VA 22217 Washington, DC 20546	10. SOURCE OF FUNDING NOS.
11 TITLE (Include Security Classification) (See page ii)	

PROGRAM ELEMENT NO.	PROJECT NO.	TASK NO.	WORK UNIT NO.
61153N	RR033-02-44	W-14365	DN330-189 DN191-108

12. PERSONAL AUTHOR(S)
Ganguli, G.,* Bakshi, P.,** and Palmadesso, P.

13a. TYPE OF REPORT	13b. TIME COVERED	14. DATE OF REPORT (Yr., Mo., Day)	15 PAGE COUNT
Interim	FROM TO	July 27, 1984	23

16. SUPPLEMENTARY NOTATION *Science Applications, Inc., McLean, VA 22102
**Department of Physics, Boston College, Chestnut Hill, MA 02167 (Continues)

17 COSATI CODES		
FIELD	GROUP	SUB. GR.

18. SUBJECT TERMS (Continue on reverse if necessary and identify by block number)
Current driven ion cyclotron instability
Finite current channel
Nonlocal plasma theory

19 ABSTRACT (Continue on reverse if necessary and identify by block number)

Nonlocal effects due to magnetic shear and finite current channel width on the convective characteristics of the current driven ion cyclotron instability have been investigated. When the magnetic shear length (L_s) is smaller than the current channel width (L_c), the group velocity parallel to the external magnetic field at the origin (V_{gz}) vanishes, and there is a reduction in the group velocity perpendicular to the external magnetic field (V_{gy}). For $L_c \sim 10^{-2} L_s$ the values of V_{gz} and V_{gy} as given by local theory are recovered. When $L_c \lesssim \rho_i$ is the mean ion Larmor radius, both V_{gz} and V_{gy} change sign, indicating a reversal of the direction of propagation.

approx 1/100 L sub S

Rho sub i

< or approx

20 DISTRIBUTION/AVAILABILITY OF ABSTRACT UNCLASSIFIED/UNLIMITED ☒ SAME AS RPT ☐ DTIC USERS ☐	21 ABSTRACT SECURITY CLASSIFICATION UNCLASSIFIED

22a NAME OF RESPONSIBLE INDIVIDUAL	22b TELEPHONE NUMBER (Include Area Code)	22c OFFICE SYMBOL
P. Palmadesso	(202) 767-6780	Code 4700.1P

DD FORM 1473, 83 APR EDITION OF 1 JAN 73 IS OBSOLETE

SECURITY CLASSIFICATION OF THIS PAGE

11. TITLE (Include Security Classification)

Nonlocal Effects on the Convective Properties of the Electrostatic Current Driven Ion-Cyclotron Instability

16. SUPPLEMENTARY NOTATION (Continued)

This work was supported by the Office of Naval Research and the National Aeronautics and Space Administration.

CONTENTS

NONLOCAL EFFECTS ON THE CONVECTIVE PROPERTIES OF THE ELECTROSTATIC CURRENT DRIVEN ION CYCLOTRON INSTABILITY

I. INTRODUCTION

The current driven ion cyclotron instability[1] (CDICI) has been of considerable interest to both space and laboratory plasma physicists for more than two decades. Recently, we have demonstrated the importance of nonlocal effects due to magnetic shear[2,3] (produced by the field aligned current) and the finite extent of the current channel[4,5]. Our past work dealing with these nonlocal aspects of the electrostatic CDICI was essentially based on a normal mode approach. The local treatment of the CDICI,[1,6,7] which assumes an infinite extent of the width of the current channel, predicts a finite group velocity of the CDICI in both the parallel and perpendicular directions relative to the external magnetic field. For a temporally growing mode, the presence or absence of a group velocity in a finite sized region of space (as opposed to a point) makes an instability convective or absolute;[8] these are two vastly different physical scenarios. This fact has been elucidated by Ashour-Abdulla and Kennel,[7] in general, and more specifically for the CDICI by Ashour-Abdulla and Thorne.[9] In our earlier work[2-4] we noted a significant difference between the local and the nonlocal results as far as growth rates of normal modes are concerned. For instabilities like the CDICI which are convective, a normal mode analysis without regard to the convective growth cannot fully determine the stability of a bounded system, and hence is somewhat limited in its application. Thus, the main objective of this paper is to report the nonlocal effects due to magnetic shear and the finite current channel width on the convective aspects of the electrostatic CDICI.

Manuscript approved April 23, 1984.

II. THEORY

In our treatment we will follow the analytical approach as given in Bakshi et al.[4] We introduce a finite current channel width in the x direction. We take the electron distribution function to be Maxwellian with a drift velocity parallel to the magnetic field which is x dependent:

$$V_d(x) = V_d^o \, g(x_g/L_c) \tag{1}$$

where $g(\xi) = \exp(-\xi^2)$ and $x_g = x + v_y/\Omega_e$. Assuming that $v_y/\Omega_e \sim O(\rho_e) << L_c$, where L_c is the characteristic length scale associated with the current channel, we approximate (1) by

$$V_d(x) = V_d^o g(x/L_c). \tag{2}$$

Using (2) and following the methods illustrated in Ref. 4 we arrive at the nonlocal, differential equation for the CDICI:

$$\left\{\left(\frac{\rho_i}{L_c}\right)^2 \frac{\partial^2}{\partial \xi^2} + Q(u, V_d)\right\} \phi(\xi) = 0, \tag{3}$$

where Q is defined by,

$$Q = -\rho_i^2 \frac{Q_1}{A}, \tag{4}$$

$$Q_1 = 1 + (k_y\lambda_i)^2 + \tau + \sum_n \Gamma_n(b)\zeta_i Z((1 - np)\zeta_i)$$

$$+ \tau\,(\zeta_e - \frac{V_d(\xi)}{v_e}) Z(\zeta_e - \frac{V_d(\xi)}{v_e}), \tag{5}$$

$$A = \frac{\rho_i^2}{2}\zeta_i \sum_n \Gamma_n'(b)\ Z((1 - np)\zeta_i), \tag{6}$$

where $b = k_y^2\rho_i^2/2$, $\Gamma_n' = \partial\Gamma_n/\partial b$, $\tau = T_i/T_e$, $p = \Omega_i/\omega$, $\zeta_i = \omega/|k_\parallel|v_i$, $\xi = x/L_c$, $\zeta_e = \omega/|k_\parallel|v_e$, $k_\parallel(x) = k_z + k_y(L_c/L_s)\int_0^\xi g(\xi)d\xi$, $u = k_\parallel(x)/k_y$ and L_s is the characteristic length associated with the shear in the magnetic field.

The dispersion equation is given by:[4]

$$Q'(\omega, \xi_1) = 0, \tag{7a}$$

$$Q(\omega, \xi_1) = (2\ell + 1)(\rho_i/L_c)[-\frac{1}{2}Q''(\omega, \xi_1)]^{1/2}, \tag{7b}$$

where Q' and Q'' are the first and second derivatives of Q with respect to ξ evaluated at ξ_1, which is defined by 7a. We solve equations 7a and 7b numerically for the complex eigenfrequencies ω, given the perpendicular wave vector k_y, the parallel wave vector at the origin k_z, and other parameters characterizing the system. For evaluating the group velocities v_{gz} and v_{gy} we take the derivatives of the real part of the eigenfrequency ω_r, with respect to k_z and k_y, respectively, i.e., V_{gz} $\Delta\omega_r/\Delta k_z$ and $V_{gy} = \Delta\omega_r/\Delta k_y$. In the x direction the wave energy is confined to the vicinity of $\xi_1 = x_1/L_c$.

Figure 1a shows the parallel group velocity normalized by the ion thermal velocity v_i versus the ratio of the current channel size L_c and the magnetic shear length L_s for three different values of L_s. Here $b = 0.6$, $\tau = 0.5$, $\mu = 1837$ and $V_d^o/v_e = 0.28$. In order to evaluate the value of $(k_y \lambda_i)^2$ we have used the parameters of Ashour-Abdulla and Thorne[9], i.e., $n_o \sim 10$ cm^{-3}, $B_o \sim 0.06$ G, and $T_i \sim 2$ eV. For the first harmonic $(k_y \lambda_i)^2 \sim 0.01$ and that term in equation (5) contributes negligibly. The most interesting result of figure 1a is that in the limit $L_c \to \infty$, $V_{gz} \to 0$. One finds that as L_c is increased beyond L_s, V_{gz} approaches zero as $(L_s/L_c)^2$. Further, when L_c is made smaller than 10^{-2} L_s the value of V_{gz} attains its local value (i.e., the value predicted by local theories[1,6]) and stabilizes at that value. However, when L_c is further reduced such that $L_c < \rho_i$, V_{gz} once again decreases.

Figure 1b is a plot of V_{gy} against L_c/L_s for the parameters of Figure 1a. Here too we find a reduction in V_{gy} in the shear dominated regime (i.e., $L_c \gtrsim L_s$) much in the same fashion as the temporal growth rate.[4] However, the difference between the local and the nonlocal values of V_{gy} is not as striking as that of V_{gz}. As noted by Ashour-Abdulla and Thorne,[9] V_{gy} for the CDICI near the dominant normal mode (which occurs for $b \sim O(1)$) is extremely small; and combined with our results that $V_{gz} \to 0$ in the nonlocal regime the CDICI becomes, effectively, an absolute instability. For $L_c < \rho_i$, V_{gy} becomes negative. Figures 2a and 2b are plots similar to 1a and 1b for the second harmonic. Here we use $\tau = 1$, $V_d^0/v_e = 0.55$ and $b = 2.4$. The value of b for all the calculations corresponds to the maximum temporal growth rate. We see trends similar to figure 1a and 1b for the higher harmonic also.

In Figure 3 we plot the convective growth rate $k_{iz} = \gamma/V_{gz}$ normalized by the mean ion Larmor radius versus L_c/L_s. We see two distinct regions joined smoothly. For very small L_c/L_s (i.e., $L_c/L_s \lesssim 10^{-3}$), $k_{iz}\rho_i < 0$ which indicates spatially damped waves. When L_c/L_s is increased the curves attain a plateau which corresponds to the local theory. Here we find a finite $k_{iz}\rho_i$ and, hence, a finite region in which the wave amplitude can be amplified by one e-fold. For $L_c \gtrsim L_s$, $k_{iz}\rho_i$ grows without bound, implying that the wave amplitude can e-fold in an insignificantly small region (Recall that the system is assumed to be infinite and uniform in the y direction, hence convection in this direction is ignorable). Thus the character of CDICI is changed from <u>convective</u> to <u>absolute</u>.

We have so far considered only one species of ions characterized by a temperature T_i. In order to make the system more realistic, especially for space applications, we added a second ion species characterized by a hotter temperature but still with a Maxwellian distribution. The general features of the group velocity behavior is still the same as in a single ion species. A more detailed parametric study of the nonlocal convective aspects of CDICI with a loss cone distribution for the hotter ion species, along with the magnetospheric application will be presented elsewhere.

III. DISCUSSION

Thus, in contrast to local theory, nonlocal theory gives zero group velocity for the CDICI along the average external magnetic field direction in the limit $L_c > L_s$. Clearly the ratio L_c/L_s is the important parameter and its magnitude must be well established before making definitive conclusions regarding the electrostatic CDICI. Depending on the value of L_c/L_s, the CDICI can be classified into three main regimes:

(i) $\underline{L_c \gtrsim 0.1\ L_s}$ This regime is purely nonlocal with a temporal growth rate much reduced from its local value. Also the instability is absolute or only very weakly convective in the z direction which is the direction of the average external magnetic field and the current flow. There is no energy flow in the x direction, and energy flow in the y direction is ignorable if $\frac{\partial}{\partial y} \equiv 0$.

(ii) $\underline{L_c < 0.01\ L_s}$ In this regime nonlocal theory reproduces the results of local theory, and the instability becomes convective in the z direction with a convective, as well as a temporal growth rate, equal to the ones given by the local theory. There is a smooth transition between regimes (i) and (ii) as is evident in all the figures.

(iii) $\underline{L_c \sim \rho_i << L_s}$ The finite channel width becomes important. There is once again a reduction in the temporal growth rate (filamental quenching[4]) but the instability remains convective, i.e., V_{gz} remains non-zero. However, when L_c is further reduced so that $L_c < \rho_i$ both V_{gz} and V_{gy} become reduced and eventually become negative.

Physically the reason for vanishing parallel group velocity can be described as follows. Figure 4 shows the angle space where the imaginary part of the local dispersion relation $D_I < 0$, and the growth rate is positive for the CDICI. The extent of this unstable angular space Δu for the CDICI in our parameter range is about 0.1. In the nonlocal theory a wave packet is formed whose size is governed by the smaller of the two scale lengths L_c and 0.1 L_s. When $L_c < 0.1\ L_s$ the drift velocity $V_d(x)$ varies sufficiently fast as a function of x, or as a function of the angle u within the space Δu, so as to form an effective Q_I curve which has the form of a steep well. The position of the bottom of this well is at $u_o = k_z/k_y$; thus different choices of k_z center the well in different parts of the region Δu and the corresponding wave packets (of size $\sqrt{\rho_i L_c}$) sample different regions of Δu which lead to different growth rates γ as well as different real frequencies ω_r. On the other hand, when $L_c > L_s$, the variation of $V_d(x)$ in the domain Δu is rather weak and the effective Q_I curve is governed by the variation of u rather than that of V_d in Eq. (3). Now, if we choose different k_z, an appropriate translation in x (i.e., moving away from the center of the slab) is sufficient to provide almost the same invariant Q_I curve as a function of u. The resulting wave packet (of size $\sqrt{\rho_i L_s}$) forms at the same position in u space (even though we choose different k_z) and has the same growth rate γ and real frequency ω_r, independent of k_z. This makes the group velocity $\partial\omega_r/\partial k_z$ vanish in the limit $L_c \rightarrow \infty$.

IV. CONCLUSION

We have shown in this paper that the nonlocal effects due to the magnetic shear (produced by a field aligned current) and a finite channel current width can drastically alter the character of the electrostatic CDICI by making the instability effectively absolute in the z direction. The important parameter turns out to be the ratio of the two scale lengths involved in the problem L_c and L_s. Depending on the value of L_c/L_s one can classify the CDICI in three regimes as described earlier, and a careful assessment of the value of L_c/L_s for a given physical situation becomes essential to draw any definitive conclusion regarding the growth and convective characteristics of the electrostatic CDICI. We would also like to note that the nonlocal effects due to magnetic shear can be expected to produce corresponding phenomena, including the vanishing of the parallel group velocity, in various other current driven instabilities as well.

ACKNOWLEDGMENTS

We would like to thank Dr. J. Huba of the Naval Research Laboratory for useful comments. This work was supported by the Office of Naval Research and the National Aeronautics and Space Administration.

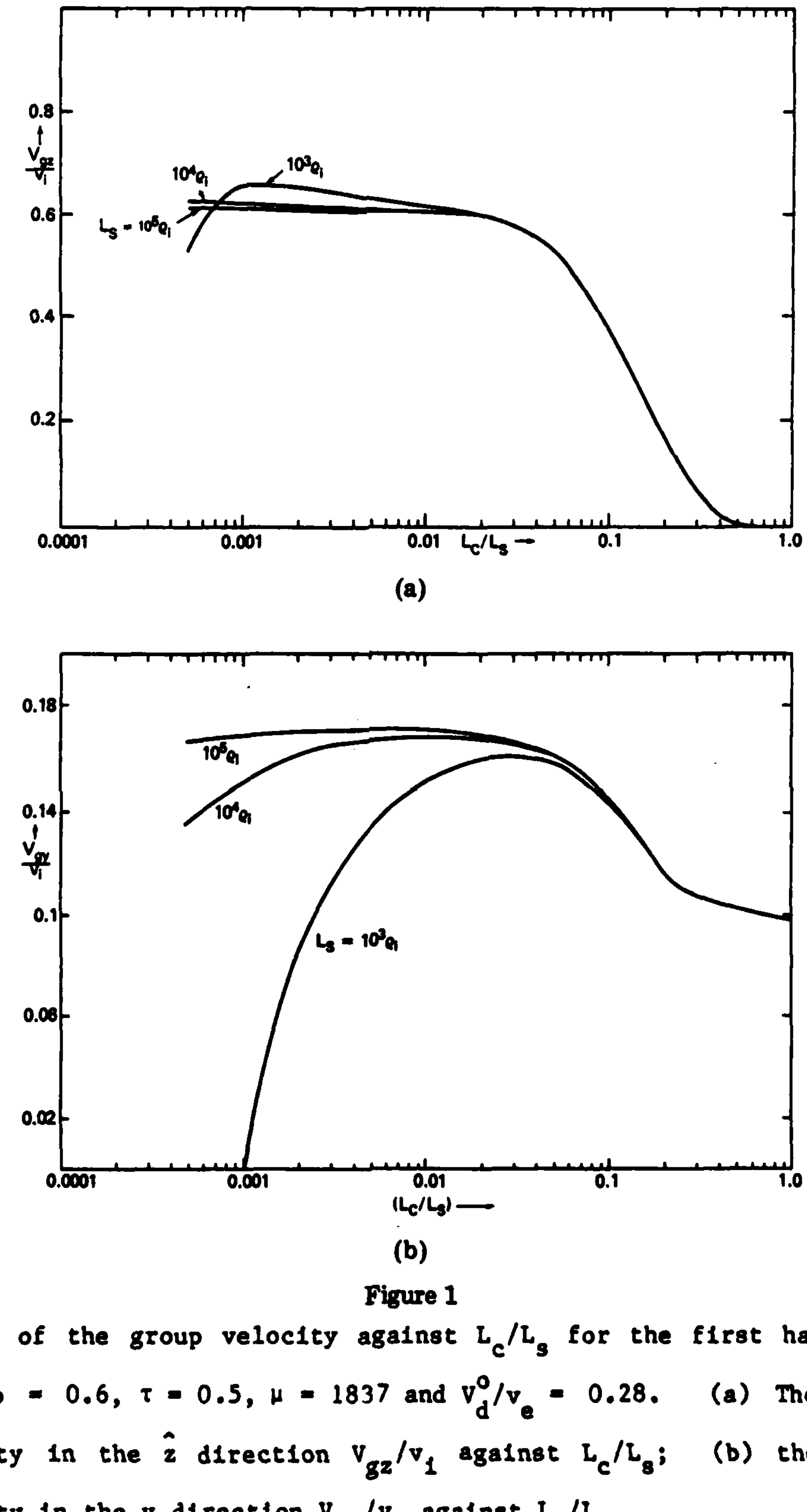

Figure 1

A plot of the group velocity against L_c/L_s for the first harmonic. Here $b = 0.6$, $\tau = 0.5$, $\mu = 1837$ and $V_d^0/v_e = 0.28$. (a) The group velocity in the $\hat{z}$ direction V_{gz}/v_i against L_c/L_s; (b) the group velocity in the y direction V_{gy}/v_i against L_c/L_s.

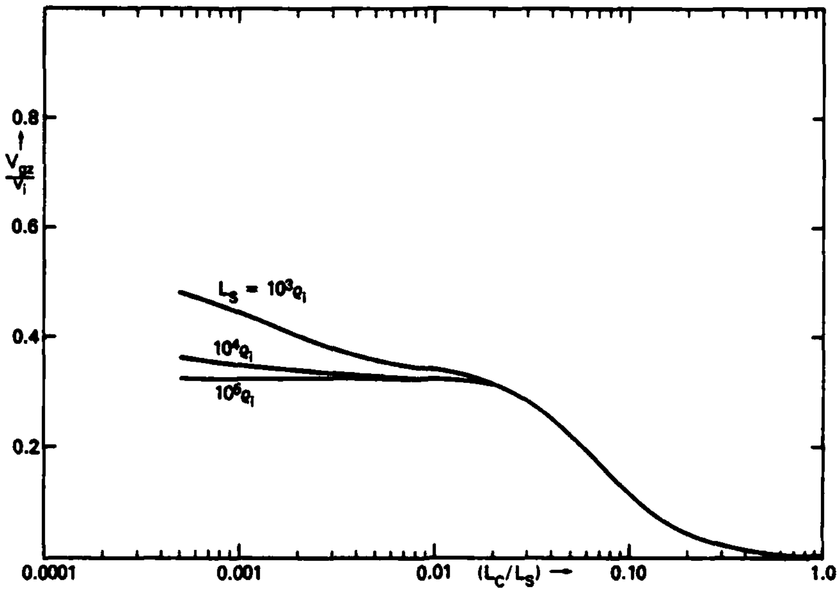

(a)

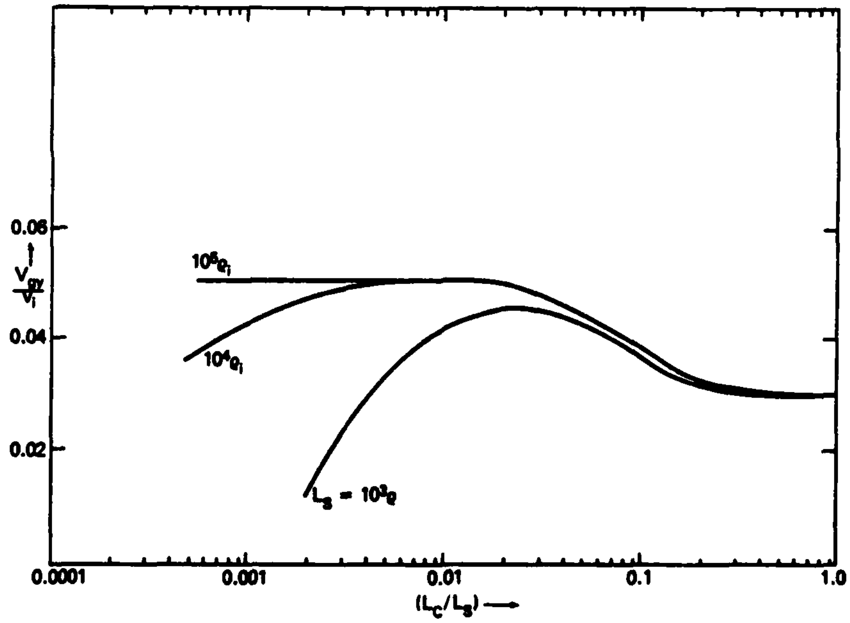

(b)

Figure 2

A plot similar to Fig. (1) for the second harmonic. Here b = 2.4, τ = 1.0, μ = 1837 and V_d^o/v_e = 0.55. (a) V_{gz}/v_i against L_c/L_s; (b) V_{gy}/v_i against L_c/L_s.

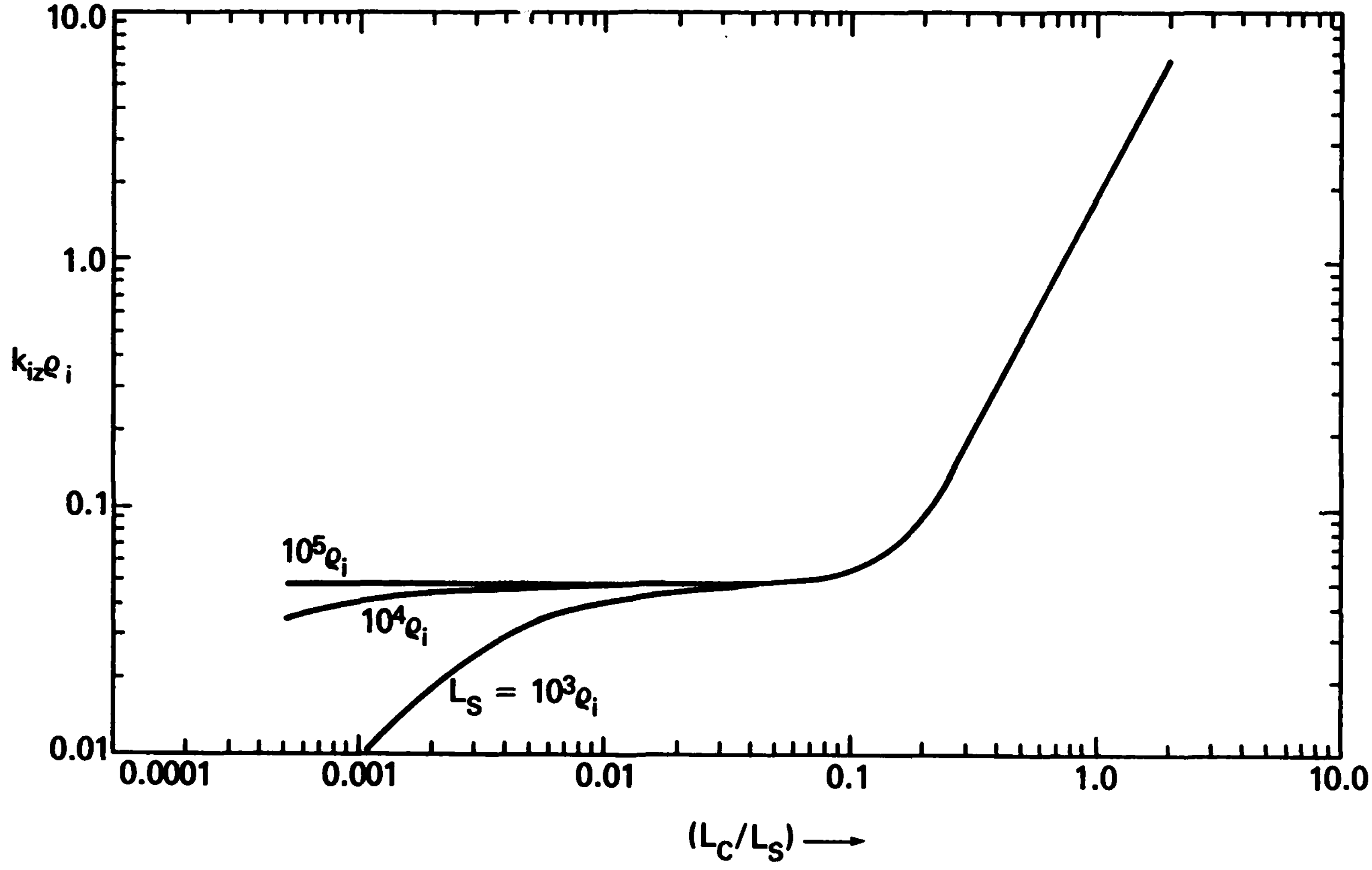

Figure 3

A plot of the convective growth rate normalized by the ion Larmor radius $k_{iz}\rho_i$ versus L_c/L_s for the first harmonic. The other parameters are identical to 1a.

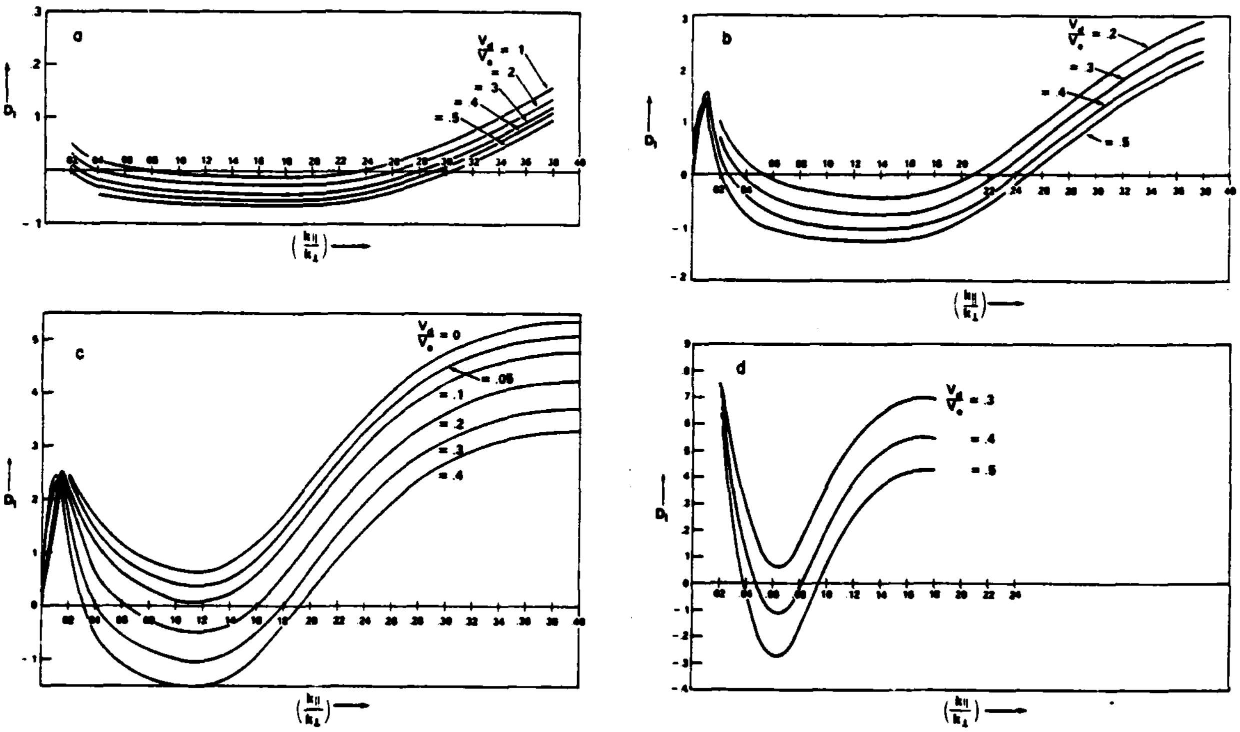

Figure 4

A plot of imaginary part of the local dispersion relation $D_I(\omega, k)$ against $k_z/k_\perp$ (reproduced from Ref. 2) for various V_d^o/v_e. Here b = 0.5, μ = 3674 and four different values of the temperature ratio τ: (a) τ = 0.1, (b) τ = 0.2, (c) τ = 0.33, and (d) τ = 1.0.

REFERENCES

(1) W.E. Drummond and M.N. Rosenbluth, Phys. Fluids 5, 1507 (1962).

(2) G. Ganguli and P. Bakshi, Phys. Fluids 25, 1830 (1982).

(3) G. Ganguli, Ph.D. Thesis, Boston College, Chestnut Hill, Mass., 1980.

(4) P. Bakshi, G. Ganguli and P. Palmadesso, Phys. Fluids 26, 1808 (1983).

(5) G. Ganguli, P. Bakshi and P. Palmadesso, J. Geophys. Res. 89, 945 (1984).

(6) J.M. Kindel and C.F. Kennel, J. Geophys. Res. 76, 3055 (1971).

(7) M. Ashour-Abdalla and C.F. Kennel, J. Geophys. Res. 83, 1531 (1978): C.F. Kennel and M. Ashour-Abdalla, Magnetospheric Plasma Physics (D. Reidel Publishing Company, 1982), p. 245.

(8) R.N. Sudan, Phys. Fluids 8, 1899 (1965).

(9) M. Ashour-Abdalla and R.M. Thorne, J. Geophys. Res. 83, 4755 (1978).

DISTRIBUTION LIST

Director
Naval Research Laboratory
Washington, D.C. 20375
ATTN: Code 4700 (26 Copies)
Code 4701
Code 4780 (100 copies)
Code 4187 (E. Szuszczewicz)
Code 4187 (P. Rodriguez)

University of Alaska
Geophysical Institute
Fairbanks, Alaska 99701
ATTN: Library
S. Akasofu
J. Kan
J. Roederer
L. Lee

University of Arizona
Dept. of Planetary Sciences
Tucson, Arizona 85721
ATTN: J.R. Jokipii

University of California, S.D.
LaJolla, California 92037
(Physics Dept.):
ATTN: J.A. Fejer
T. O'Neil
J. Winfrey
Library
J. Malmberg
(Dept. of Applied Sciences):
ATTN: H. Booker

University of California
Los Angeles, California 90024
(Physic Dept.):
ATTN: J.M. Dawson
B. Fried
J.G. Moralles
W. Gekelman
R. Stenzel
Y. Lee
A. Wong
F. Chen
M. Ashour-Abdalla
Library
J.M. Cornwall

(Institute of Geophysics and
Planetary Physics):
ATTN: Library
C. Kennel
F. Coroniti

Columbia University
New York, New York 10027
ATTN: R. Taussig
R.A. Gross

University of California
Berkeley, California 94720
(Space Sciences Laboratory):
ATTN: Library
M. Hudson
(Physics Dept.):
ATTN: Library
A. Kaufman
C. McKee
(Electrical Engineering Dept.):
ATTN: C.K. Birdsall

University of California
Physics Department
Irvine, California 92664
ATTN: Library
G. Benford
N. Rostoker
C. Robertson
N. Rynn

California Institute of Technology
Pasadena, California 91109
ATTN: R. Gould
L. Davis, Jr.
P. Coleman

University of Chicago
Encrico Fermi Institute
Chicago, Illinois 60637
ATTN: E.N. Parker
I. Lerche
Library

Thayer School of Engineering
Dartmouth College
Hanover, NH 03755
ATTN: Bengt U.O. Sonnerup

University of Colorado
Dept. of Astro-Geophysics
Boulder, Colorado 80302
ATTN: M. Goldman
Library

Cornell University
School of Applied and Engineering Physics
College of Engineering
Ithaca, New York 14853
ATTN: Library
R. Sudan
B. Kusse
H. Fleischmann
C. Wharton
F. Morse
R. Lovelace

Harvard University
Cambridge, Massachusetts 02138
ATTN: Harvard College Observatory
(Library)
G.S. Vaina
M. Rosenberg

Harvard University
Center for Astrophysics
60 Garden Street
Cambridge, Massachusetts 02138
ATTN: G.B. Field

University of Iowa
Iowa City, Iowa 52240
ATTN: C.K. Goertz
D. Gurnett
G. Knorr
D. Nicholson

University of Houston
Houston, Texas 77004
ATTN: Library

University of Maryland
Physics Dept.
College Park, Maryland 20742
ATTN: K. Papadopoulos
H. Rowland
C. Wu

University of Michigan
Ann Arbor, Michigan 48140
ATTN: E. Fontheim

University of Minnesota
School of Physics
Minneapolis, Minnesota 55455
ATTN: Library
J.R. Winckler
P. Kellogg

M.I.T.
Cambridge, Massachusetts 02139
ATTN: Library
(Physics Dept.):
ATTN: B. Coppi
V. George
G. Bekefi
T. Dupree
R. Davidson
(Elect. Engineering Dept.):
ATTN: R. Parker
A. Bers
L. Smullin
(R.L.E.):
ATTN: Library
(Space Science):
ATTN: Reading Room

Princeton University
Princeton, New Jersey 08540
Attn: Physics Library
Plasma Physics Lab. Library
C. Oberman
F. Perkins
T.K. Chu
H. Okuda
V. Aranasalan
H. Hendel
R. White
R. Kurlsrud
H. Furth
S. Yoshikawa
P. Rutherford

Rice University
Houston, Texas 77001
Attn: Space Science Library
R. Wolf

University of Rochester
Rochester, New York 14627
ATTN: A. Simon

Stanford University
Institute for Plasma Research
Stanford, California 94305
ATTN: Library

Stevens Institute of Technology
Hoboken, New Jersey 07030
ATTN: B. Rosen
G. Schmidt
M. Seidl

University of Texas
Austin, Texas 78712
ATTN: W. Drummond
V. Wong
D. Ross
W. Horton
D. Choi
R. Richardson
G. Leifeste

College of William and Mary
Williamsburg, Virginia 23185
Attn: F. Crownfield

Lawrence Livermore Laboratory
University of California
Livermore, California 94551
ATTN: Library
B. Kruer
J. Thomson
J. Nucholls
J. DeGroot
L. Wood
J. Emmett
B. Lasinsky
B. Langdon
R. Briggs
D. Pearlstein

Los Alamos National Laboratory
P.O. Box 1663
Los Alamos, New Mexico 87545
ATTN: Library
D. Forslund
J. Kindel
B. Bezzerides
H. Dreicer
J. Ingraham
R. Boyer
C. Nielson
E. Lindman
L. Thode

N.O.A.A.
325 Broadway S.
Boulder, Colorado 80302
ATTN: J. Weinstock
Thomas Moore (SEL, R-43)
W. Bernstein
D. Williams

Sandia Laboratories
Albuquerque, New Mexico 87115
ATTN: A. Toepfer
G. Yeonas
D. VanDevender
J. Freeman
T. Wright

Bell Laboratories
Murray Hill, New Jersey 07974
ATTN: A. Hasegawa

Lockheed Research Laboratory
Palo Alto, California 94304
ATTN: M. Walt
J. Cladis
J. Siambis

Physics International Co.
2400 Merced Street
San Leandro, California 94577
ATTN: J. Benford
S. Putnam
S. Stalings
T. Young

Science Applications, Inc.
Lab. of Applied Plasma Studeis
P.O. Box 2351
LaJolla, California 92037
ATTN: L. Linson
J. McBride

NASA/Goddard Space Flight Center
Greenbelt, Maryland 20771
ATTN: M. Goldstein
T. Northrop
T. Birmingham

NASA/Goddard Space Flight Center
Greenbelt, MD 20771
ATTN: A. Figuero Vinas
Code 692

TRW Space and Technology Group
Space Science Dept.
Building R-1, Room 1170
One Space Park
Redondo Beach, California 90278
ATTN: R. Fredericks
W.L. Taylor

National Science Foundation
Atmospheric Research Section (ST)
Washington, D.C. 20550
ATTN: D. Peacock

Goddard Space Flight Center
Code 961
Greenbelt, Maryland 20771
ATTN: Robert F. Benson

NASA Headquarters
Code EE-8
Washington, D.C. 20546
ATTN: Dr. E. Schmerling
Dr. J. Lynch
Dr. D. Butler

Klumpar, David
Center for Space Sciences
P.O. Box 688
University of Texas
Richardson, Texas 75080

Leung, Philip
Dept. of Physics
University of California
405 Hilgard Avenue
Los Angeles, California 90024

Lysak, Robert
School of Physics and Astronomy
University of Minnesota
Minneapolis, MN 55455

Schulz, Michael
Aerospace Corp.
A6/2451, P.O. Box 92957
Los Angeles, California 90009

Shawhan, Stanley
Dept. of Physics & Astronomy
University of Iowa
Iowa City, Iowa 52242

Temerin, Michael
Space Science Lab.
University of California
Berkeley, California 94720

Vlahos, Loukas
Dept. of Physics
University of Maryland
College Park, Maryland 20742

Matthews, David
IPST
University of Maryland
College Park, Maryland 20742

Schunk, Robert W.
Utah State University
Dept. of Physics
Logan, Utah 84322

Director,
Department of Energy
ER20:GTN, High Energy &
Nuclear Physics
Washington, D.C. 20545
ATTN: Dr. Terry Godlove

Director,
Department of Energy
Office of Inertial Fusion
Washington, D.C. 20545
ATTN: Dr. Richard Schriever

Director
Defense Nuclear Agency
Washington, D.C. 20305
ATTN: Dr. Leon Wittwer
Dr. P. Crowley
Dr. Carl Fitz

FILMED

9-81